

# Chemical bonding analysis of electron-sensitive polymers by EELS

K. Varlot<sup>a,\*</sup>, J.M. Martin<sup>a</sup>, D. Gonbeau<sup>b</sup>, C. Quet<sup>c</sup>

<sup>a</sup>*Ecole Centrale de Lyon, Laboratoire de Tribologie et Dynamique des Systèmes, UMR 5513, BP 163, 69131 Ecully cedex, France*

<sup>b</sup>*Université de Pau et des Pays de l'Adour, Laboratoire de Physico-Chimie Moléculaire UMR 5624, avenue de l'université, 64000 Pau, France*

<sup>c</sup>*Elf Atochem, Groupement de Recherches de Lacq, BP 34, 64170 Artix France*

Received 28 April 1998; received in revised form 26 October 1998; accepted 26 October 1998

## Abstract

We have performed EELS analysis of poly(methyl metacrylate) (PMMA) in the analytical TEM in order to evaluate the possibility to obtain chemical information on electron sensitive polymers. In the acquired spectra, we propose an identification to the different chemical bondings in agreement with molecular orbital calculations and with previous XANES experiments. Moreover, main results confirm that PMMA is very sensitive to electrons with a critical dose of about  $10^2 \text{ C m}^{-2}$ . The evolution of the EELS spectra of PMMA during irradiation damage is found to be slightly dependant on the molecular weight of the polymer. Finally, a degradation process in agreement with EELS data is proposed. © 1999 Elsevier Science Ltd. All rights reserved.

*Keywords:* EELS; Polymer; Molecular orbital

## 1. Introduction

Electron Energy-Loss Spectroscopy (EELS) in the Transmission Electron Microscope (TEM) is a very powerful technique for measuring the spectrum of electronic excitations in various materials, including amorphous ones. Spectra can be recorded over the entire energy range of valence and core electronic excitations, with a very high spatial resolution (down to 0.5 nm probe size with an electron microscope equipped with a field-emission gun). This can be very useful to solve problems for example in the field of composite material interfaces.

As far as polymers are concerned, their high sensitivity to the electron beam requires particular attention to experimental conditions, in order to the characteristic excitation spectrum before significant damage occurs. This also implies the analysis of the degradation process with the evolution of the chemical bondings. X-ray Absorption Spectroscopy (XAS), the technique using the synchrotron radiation which is theoretically equivalent to EELS, produces spectra which can be viewed as references since the energy resolution is far better and since the irradiation damage are about three orders of magnitude less than in TEM/EELS.

Poly(methyl metacrylate) (PMMA), widely used in the lithographic process of the fabrication of microcircuits, is known as one of the most sensitive polymers to the electron

beam. It has already been extensively studied by low-loss EELS [1] and XAS [2], but there are still some questions particularly concerning the energy of the CO chemical bonding transitions and the existence of a  $\sigma^*(\text{C-H})$  excitation. The aim of this article is first to precisely identify the chemical bondings of PMMA from the EELS spectrum, and second to study the degradation process in function of the molecular weight of the polymer.

## 2. Effect of irradiation on polymers

Radiation affects materials by the energy transfer between the incident electron and the atoms of the material. A large number of very rapid processes can occur. If the energy is higher than about 10–15 eV, an electron from the material will be expelled from its orbit, creating a positive ion rapidly dissociating into free radicals or molecular fragments. Further chemical changes result from the movement of the free radicals. The recombination occurs at a rate controlled by the type of electron trap and by the temperature of the specimen [3,4].

The exact nature of the irradiation product will depend not only on the elemental composition but also on molecular configuration, conformation and size. The energy transfer and the very different sensitivities of chemical structures result in specific bonds or types of bonds being preferentially disrupted. The bonds broken need not to be those least stable energetically: for example,  $\sigma(\text{C-H})$  is one of the

\* Corresponding author. Tel.: 0033 4 7218 6298; fax: 0033 4 7843 3383.

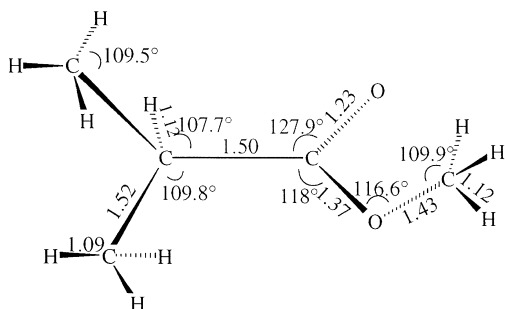


Fig. 1. Geometry of methyl methacrylate after optimisation of the total energy of the molecule.

most sensitive chemical bond whereas it is far more stable than  $\sigma(\text{C}-\text{C})$ . This is owing to the delocalization of the excitation along the backbone chain when the excitation concerns a  $\sigma^*(\text{C}-\text{C})$  bond but not a  $\sigma^*(\text{C}-\text{H})$  [5].

All poly(metacrylates) and their copolymers are known to undergo chain scission of the main chain and of the side groups with gas liberation when irradiated [6]. Such a degradation process should then induce differences in kinetics as far as PMMA with different molecular weights are concerned.

### 3. Experimental conditions and treatment of the data

#### 3.1. EELS spectra

Pellets of PMMA with two different molecular weights ( $M_w = 1.5 \cdot 10^5$  and  $3 \cdot 10^6$ ) were microtomed at room temperature (Ultracut E from Reichert–Jung). The sections of about 50 nm thick were placed on top of 400-mesh copper grids covered by a holey carbon film. During all EELS analyses, the specimen was maintained at low temperature, typically 117 K using liquid nitrogen cooler. There are indeed less irradiation damage at low temperature since secondary reactions are inhibited [7]. Moreover, cooling down to liquid nitrogen temperature avoids specimen contamination by limiting motion of adsorbed molecules on the solid surface

Sequences of EELS spectra from a same polymer area were performed on a TEM operating at 120 kV accelerating voltage (Philips EM-420) with an under-saturated  $\text{LaB}_6$  filament, equipped with a post-column parallel energy-loss spectrometer (Gatan PEELS 666) placed under the column. The energy resolution was measured to be 1.1 eV FWHM on the zero-loss peak, and the collection angle was set at 9.48 mrad. Typically, the acquisition time necessary to get a good signal/noise ratio is about 1 s for carbon and oxygen K-edge spectra. The probe diameter is approximately 1  $\mu\text{m}$ , so that EELS spectra with electron doses below  $10^3 \text{ C m}^{-2}$  are possible to acquire in this configuration (low-loss or quantitative spectra). Higher electron doses require more

acquisition time only, the settings of the electron gun being kept constant during all experiments.

For a chemical characterization of PMMA using EELS, we focus the carbon and the oxygen K-edges. The near-edge structure (ELNES) reflects indeed the distribution of density of unoccupied levels (signature of chemical bondings and hybridization states). They are representative of the chemical structure of the polymer. Moreover, the relative intensities under each edge give the O/C atomic ratio of the molecule.

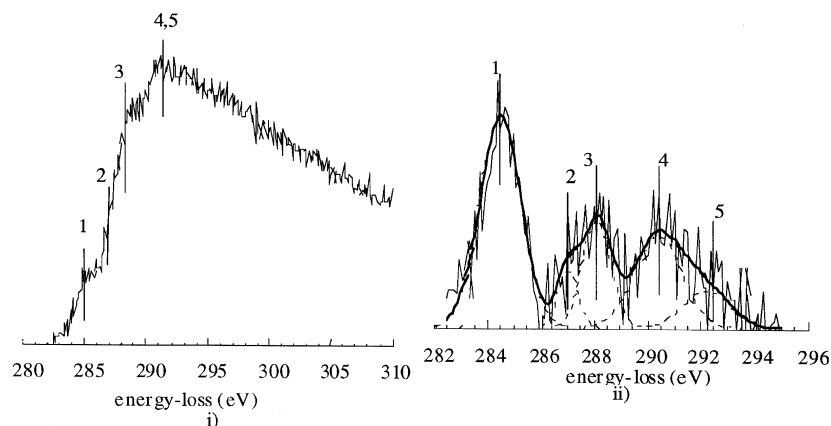
As we use TEM, conventional imaging of the irradiated area can also give interesting insight in any thickness change (or bubbling) inside the specimen.

We developed a home-made user-friendly software using Labview graphical programming language. Spectra are first corrected by the corresponding dark noise and gain variations. The edges are then extracted and deconvolved using the Fourier-ratio method. Lastly, the ionization continuum subtraction using a four-parameter function [8] and the decomposition of the extracted signal in gaussian functions are performed. The four-parameter function was fitted to the experimental spectrum (general shape) and particularly on a region where the ELNES signal is assumed to be negligible. The decomposition into gaussian functions is performed using a chi squared minimisation similar to XPS peak fitting, excepted that the FWHMs of the gaussian functions are supposed to be independant from each other. From a theoretical point of view, they are indeed related not only to the time of life of the initial state but also of the final state. The areas under each gaussian function are calculated but do not represent anything physical. In fact, in order to quantify the ratio of chemical bondings, cross-sections related to these particular transitions should be calculated. All parts of the treatment are processed in the most accurate way by moving in real time the parameters, calculating and displaying both the function and the related  $\chi^2$

#### 3.2. Molecular orbital calculations

We performed molecular orbital calculations using the Extended Hückel Theory (EHT) in order to precisely assign the peaks extracted from the EELS spectra at the C and O K-edges and then decomposed into gaussian functions. The molecule was chosen to be the monomer since no conjugation over several monomer units were expected. Terminations were set to be H atoms, their influence on the final result being however negligible.

The geometry of the molecule was optimised so that its energy was as low as possible. The resulting geometry is displayed in Fig. 1. The calculation of the excited states was performed using the equivalent ionic core virtual orbital model (EICVOM), replacing for each inequivalent site an atom Z by an atom  $Z + 1$ . The excitation of the  $\text{C}^*\text{H}_3$  carbon, which corresponds to the terminations of the molecule, will not be taken into account since such a carbon does not exist in the polymer.



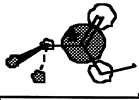



peak	energy (eV)	indexation	molecular orbital representation
1	284.8	$\pi^*(C=C)$	comparison with other polymers
2	287.3	Rydberg/ $\sigma^*(C-H)$	ab initio calculations [12].
3	288.4	$\pi^*(COO)$	
4	290.8	$\sigma^*(C-O-C)$	
5	292.8	$\sigma^*(C-C)$	
XANES	295.6	mixed, but mainly $\sigma^*(C-O-C)$	

Fig. 2. i) EELS spectra of PMMA at the carbon K-edge with ii) the decomposition of the ELNES signal after subtraction of the ionisation continuum. The peaks were assigned in agreement with EHT calculations summed up in the table below the EELS spectra. The first peak at 284.8 eV is assigned to a  $\pi^*(C=C)$  created under irradiation and therefore was ignored in the EHT calculations. Moreover, peak 3 at 287.4 eV could not be accounted for and was then assigned to a  $1s \rightarrow$  Rydberg/ $\sigma^*(C-H)$  transition in agreement with ab initio calculations.

As the energy of the molecular orbital refers to the Ionization Potential (IP) of the excited atoms, an absolute calibration was set using the IPs measured by XPS in gas phase [9]. For each excited state, the energy 0 is associated to the corresponding IP. All orbitals are then displayed on the same diagram. For each molecular orbital, a weight is calculated using  $(\sum c^2(X_{2p}))$ , sum of the coefficients of the atomic orbitals of nitrogen (or fluorine). This weight can be viewed as the probability to obtain this particular transition. In the following discussion, only molecular orbitals with a weight greater than 0.1 will be considered.

Unfortunately, the values of the IPs differ from the gas phase to the polymer for different reasons:

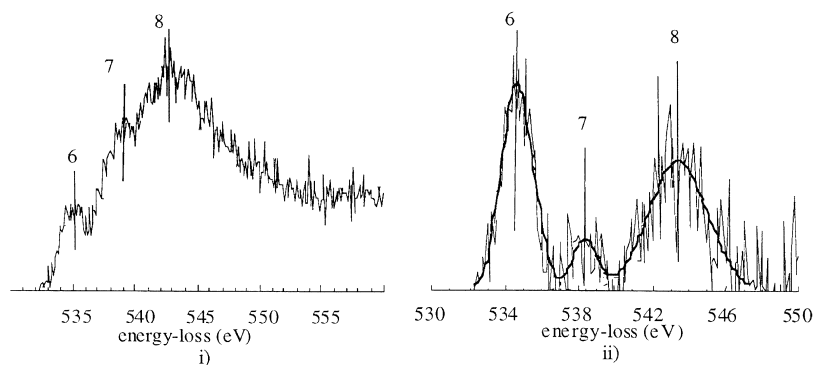
- the reference is the Fermi level which is typically 4 eV below the vacuum level, which is the reference in XPS.
- the delocalisation of the excitations in the polymer may affect the energies of the excited states.
- relaxation processes are different in gas phase and in solids because of differences in the electronic density, which can affect the bonding energy.

The energy diagram is therefore calibrated again, in function of the experimental EELS spectrum: the lowest (non-negligible) orbital is set to be equal to the first peak of the spectrum, the whole diagram being translated from this value [10].

## 4. Results and discussion

### 4.1. Identification of the chemical bondings

The EELS spectrum at the carbon K-edges is displayed in Fig. 2 i). Several features in the fine structure can be distinguished, superimposed on the ionisation continuum, see Fig. 2 ii) after subtraction of the ionisation continuum. The assignment of the peaks was made with EHT calculations. The first peak is assigned in comparison to the EELS spectra of various polymers to a  $1s \rightarrow \pi^*(C=C)$  transition, which is characteristic of irradiation damage since no C=C bond exist in non-degraded PMMA. Moreover, EHT calculations could not account for the second peak at 287.3 eV, which



peak	energy (eV)	indexation	molecular orbital representation
6	534.7	$\pi^*(\text{COO})$	
7	538.4	$\sigma^*(\text{C-O-C})$	
8	543.3	$\sigma^*(\text{COO})?$	Not precise enough

Fig. 3. i) EELS spectra of PMMA at the carbon K-edge with ii) the decomposition of the ELNES signal after subtraction of the ionisation continuum. The peaks were assigned in agreement with EHT calculations summed up in the table below the EELS spectra. Unfortunately, the EHT calculations are not precise enough to assign the third peak at 543.3 eV, which is far above the IP.

was then assigned from the literature to a mixed  $1s \rightarrow$  Rydberg/ $\sigma^*(\text{C-H})$

As expected, EHT calculations show that the ELNES fine structure is composed first from transitions towards  $\pi^*$  orbitals and then towards  $\sigma^*$  ones. The only exception is  $\sigma^*(\text{C-H})$ , surrounded by  $\sigma^*$  excitations, which is owing to its mixed Rydberg character. The peak at 288.4 eV is assigned to a transition towards a  $\sigma^*$  orbital delocalized on the carbonyl function, further called  $\sigma^*(\text{COO})$ . Then the peaks at 290.8 and 292.8 eV obtained from the decomposition can respectively be assigned to  $\sigma^*(\text{C-O-C})$  and  $\sigma^*(\text{C-C})$  orbitals. Finally, the peak observed at 295.6 eV in XANES but not in EELS because of thickness effects could be assigned to a mixed but mainly  $\sigma^*(\text{C-O-C})$  orbital.

Surprisingly,  $\pi^*(\text{C=C})$  excitation dominates the fine structure whereas  $\pi^*(\text{C=O})$  was expected from XANES spectra to be preponderant. This confirms the fact that it is

impossible to acquire an EELS spectrum of PMMA at the carbon K-edge (and a fortiori at the oxygen K-edge) without irradiation damage, but this does not mean that the molecule is completely destroyed by the electron beam, the  $\pi^*(\text{C=C})$  cross section being thought to be far greater than  $\pi^*(\text{COO})$  and  $\pi^*(\text{C-H})$  ones. Further studies should calculate these cross-sections at the very beginning of the irradiation process.

Moreover, the quantification of the EELS spectrum gives an O/C atomic ratio equal to  $0.4 \pm 0.02$ , which shows that no scission of the ester group has already occurred, but main chain scissions.

At the oxygen K-edge, the EELS spectrum is displayed in Fig. 3 i) and the corresponding extracted fine structure in Fig. 3 ii). The fine structure is dominated by only three peaks. The first ones are respectively assigned to  $\pi^*(\text{COO})$  and  $\sigma^*(\text{C-O-C})$  orbitals from EHT. Unfortunately, the calculations are not precise enough to provide a good assignation of the third peak, which is therefore thought to be related to a  $\text{O}1s \rightarrow \sigma^*(\text{COO})$  transition in respect to the relative position of  $\pi^*$  and  $\sigma^*$  orbitals.

From the re-calibration of the orbital energy diagram with the experimental peaks, we deduced values for the carbon IPs in PMMA. Bond lengths of C–C and C–O chemical bonds were then calculated using an empirical law [12], see Table 1. The length of the C–O bond is in agreement with the optimized geometry of methyl methacrylate. On the contrary, the length of the C–C bond is lower than in methyl methacrylate (relative error: 8%), which is because either to an error in the re-calibration of the IP or in a reduction of the bond length owing to polymerisation.

Table 1

Bond lengths measured from the EELS spectrum of PMMA [12] and compared to the ones optimized during the molecular orbital calculation. The IPs were chosen from gas phase XPS spectra [9] and then were translated to fit the experimental EELS spectrum. The bond lengths measured by EELS are found in agreement with the calculations, the relative error ( $\Delta/d$ ) remaining less than 10%

Chemical bonding	IP (eV)	Bond length (Å) from EELS spectra	Bond length (Å) from EHT calculations	Relative error (%)
C–O	298.2	1.36	1.37	1
C–C	294.65	1.38	1.50	8

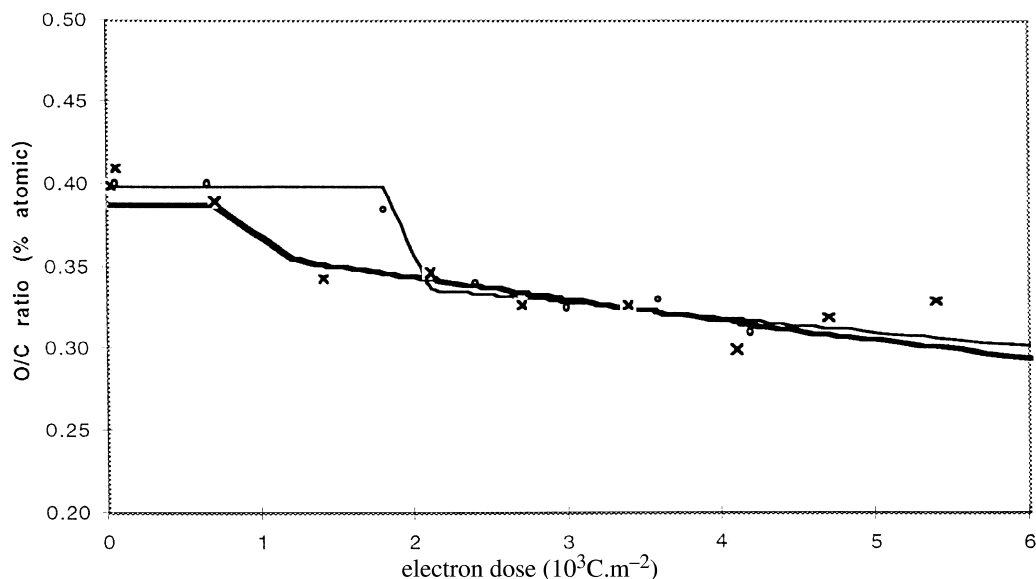


Fig. 4. Evolution of the atomic O/C ratio in PMMA in function of the electron dose. The experimental values (o for the PMMA high weight and x for the PMMA low weight) are fitted with the sum of two exponential decays modelling the loss of oxygen during the degradation process. Before a critical dose, no degradation is found, the O/C ratio remaining close to the theoretical value (0.40). The critical dose depends on  $M_w$ : the greater the molecular weight, the greater the critical dose.

#### 4.2. Degradation

Fig. 4 shows the evolution of the O/C ratio in PMMA during electron irradiation. A critical dose  $d_c$  under which the O/C ratio remains equal to 0.40 (theoretical value for non-degraded PMMA) is found to be dependant of the molecular weight, increasing with  $M_w$ . This is certainly because of a better energy transfer with a great molecular weight [5]. Above  $d_c$ , the O/C ratio was fitted with a sum of two exponential functions modelling the degradation process: the

first one refers to removal of the ester group from direct interaction with the incident electron, whereas the second one refers to a rearrangement of the excitation along the backbone. The limit of the O/C ratio for infinite electron dose is found to be close to 0.12, which means that about 80% of the ester groups were removed during irradiation.

The evolution of the ELNES fine structure at the oxygen K-edge under electron beam is displayed in Fig. 5. The characteristics of the peaks (energy, FWHM and relative area) are found to be independant on the electron dose,

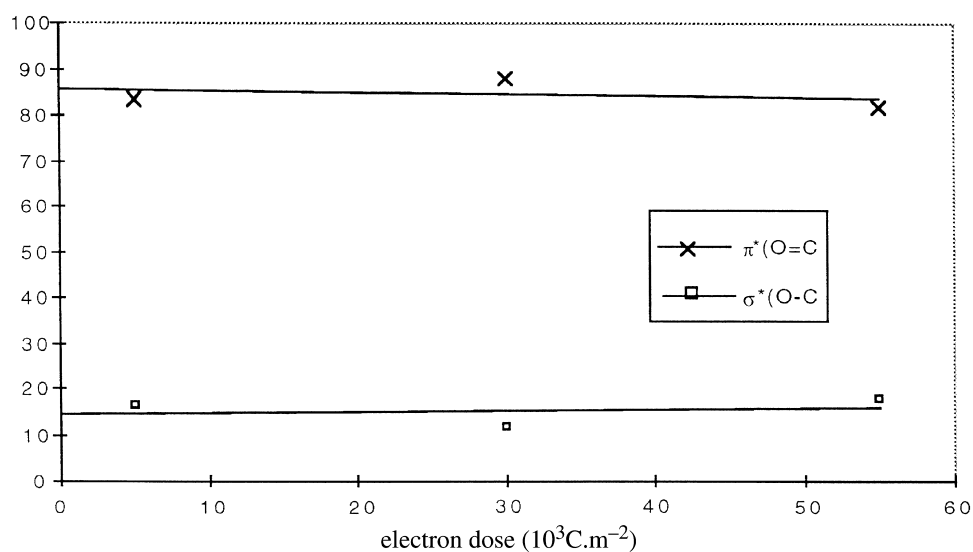


Fig. 5. Evolution of the chemical bondings at the oxygen K-edge in PMMA under electron beam. The percentage refers to the area under one gaussian curve divided by the sum of the areas under all gaussian curves and not a physical percentage of chemical bondings in the molecule. With increasing electron dose, no change is detected in the ester group. This is consistent with liberation of  $\text{HCO}_2\text{CH}_3$  detected by gaz analysis [6].

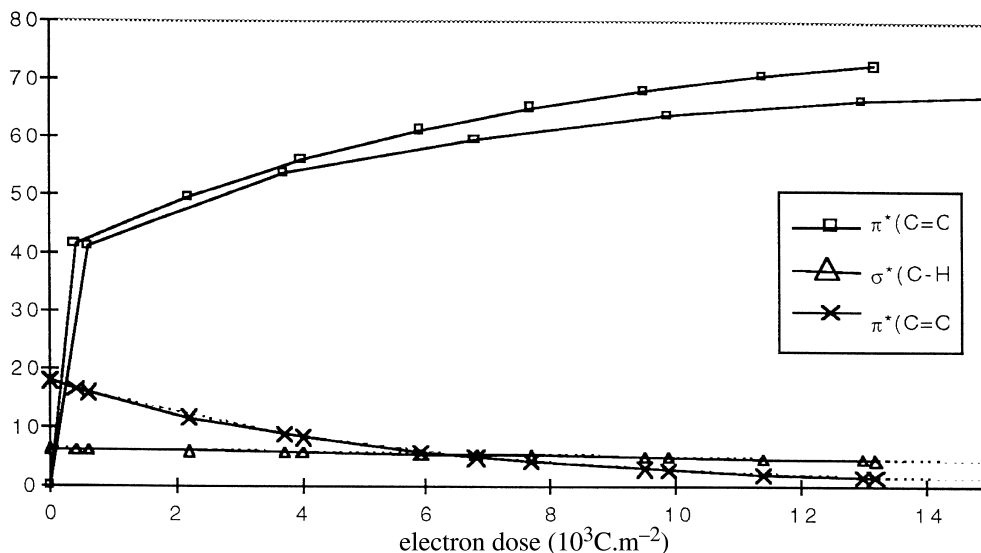


Fig. 6. Evolution of the chemical bondings at the carbon K-edge in PMMA under electron beam, in function of the molecular weight of the polymer. The percentage refers to the area under one gaussian curve divided by the sum of the areas under all gaussian curves and not a physical percentage of chemical bondings in the molecule. The experimental data were fitted by a sum of two exponential functions modelling the degradation process: the first one refers to bond breakage by direct interaction with the incident electron and the second one to reorganisation along the backbone. With increasing molecular weight, the  $1s \rightarrow \pi^*(\text{C}=\text{C})$  transition at 284.8 eV, which is characteristic of the irradiation damage, is found to increase more slowly. This is mainly owing to a better reorganisation of the excitation along the backbone, which is longer. As far as  $1s \rightarrow \sigma^*(\text{C}-\text{H})$  and  $1s \rightarrow \pi^*(\text{C}=\text{O})$  are concerned, no change was detected because of the low percentage of these peaks.

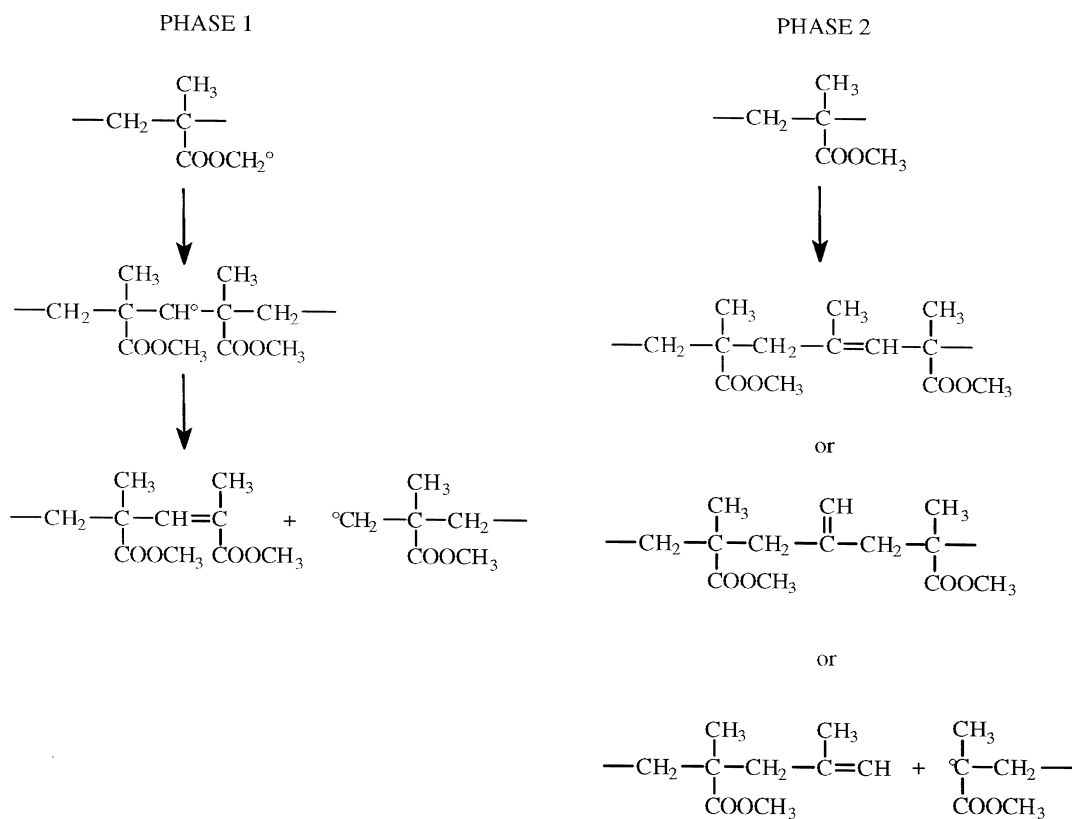


Fig. 7. Degradation process of PMMA under electron irradiation. Main chain scission without ether group removal occurs in phase 1, whereas ether group removal with dehydrogenation and formation of C=C double bonds occurs in phase 2. Phase 2 begins at a critical dose which depends on the molecular weight of the polymer.

which confirms the fact that bond scissions occur between the backbone and the ether group and not inside the ether group.

Fig. 6 shows the evolution of the chemical bondings of carbon in PMMA, in function of the molecular weight of the polymer. The experimental data are again fitted with a sum of two exponential functions. The first exponential reflects a very important creation of C=C bonds. As it occurs for low electron doses, this can be explained by main chain scissions. This phase of the degradation process is dependent on the molecular weight since the energy transfer can be trapped by chain terminations, which scission is about seven times greater than the chain's one [5]. This additional mechanism had already been proposed elsewhere [11].

The second phase of the degradation process includes the removal of the ether group with further formation of C=C double bonds by dehydrogenation. Unfortunately, the areas under the  $\pi^*(\text{C}=\text{O})$  and the  $\sigma^*(\text{C}-\text{H})$  peaks are too weak to reveal this phase of the degradation process.

The degradation process is summed up in Fig. 7. Main chain scission without ether group removal occurs in phase 1, whereas ether group removal with dehydrogenation and formation of C=C double bonds occurs in phase 2.

## 5. Conclusion

In the analytical TEM, we have performed EELS analysis of one of the most electron-sensitive polymers -poly(methyl metacrylate) (PMMA)- in order to evaluate the possibility to obtain chemical information on sensitive polymers in general. Despite some unavoidable irradiation damage, the different chemical bondings are characterised in agreement

with molecular orbital calculations and with previous XANES experiments. This makes us confident for the chemical characterisation of polymers even at high spatial resolution, which would be very useful in the field of composites.

Moreover, main results confirm that PMMA is very sensitive to electrons with a critical dose of about  $10^2 \text{ C m}^{-2}$  at 77 K. Spectra of PMMA at the carbon K-edge can therefore be acquired with a sufficient signal/noise ratio before great irradiation damage occurs. The evolution of the EELS spectra of PMMA during irradiation damage is found to be slightly dependant on the molecular weight of the polymer, and particularly during the main chain scission phase. A degradation process in agreement with EELS data is proposed.

## References

- [1] Ritsko JJ, Brillson LG, Bigelow RW, Fabish TJ. *J Chem Phys* 1978;69(9):3931.
- [2] Kikuma J, Tonner B. *J Electron Spectrosc Rel Phenom* 1996;82:53.
- [3] Grubb DT. *J Mat Sci* 1974;9:1715.
- [4] Chapiro A. *J Chim Phys* 1956;53:306.
- [5] Partridge RH. *J Chem Phys* 1970;12(5):2485–2510.
- [6] Hiraoka H. *IBM J Res and Dev* 1977;21:121.
- [7] Box HC. *Physical aspects of electron microscopy and microbeams analysis*. New York: Wiley, 1975.
- [8] Varlot K, Martin JM. *Surf Int Anal*, accepted.
- [9] Jolly WL, Bomben KD, Eyermann CY. *At Data Nucl Data Tab* 1984;31: 433–493.
- [10] Hitchcock AP, Urquhart SG, Rightor EG. *J Phys Chem* 1992;96:8736.
- [11] Kircher FJ, Sliemers FA, Markle RA, Gager WB, Leininger RI. *J Phys Chem* 1965;69:189.
- [12] Sette F, Stöhr J, Hitchcock AP. *J Chem Phys* 1984;81(1):4906–4914.